Multiscale Computational Modeling Reveals a Critical Role for TNF- α Receptor 1 Dynamics in Tuberculosis Granuloma Formation

Mohammad Fallahi-Sichani, Mohammed El-Kebir, Simeone Marino, Denise E. Kirschner and Jennifer J. Linderman

J Immunol 2011;186;3472-3483; Prepublished online 14 February 2011;
doi:10.4049/jimmunol.1003299
http://www.jimmunol.org/content/186/6/3472

The Journal of Immunology is published twice each month by
The American Association of Immunologists, Inc.,
9650 Rockville Pike, Bethesda, MD 20814-3994.

Print ISSN: 0022-1767 Online ISSN: 1550-6606.

Multiscale Computational Modeling Reveals a Critical Role for TNF-α Receptor 1 Dynamics in Tuberculosis Granuloma Formation

Mohammad Fallahi-Sichani,* Mohammed El-Kebir,[†,‡,§] Simeone Marino,[†] Denise E. Kirschner,[†] and Jennifer J. Linderman*

Multiple immune factors control host responses to *Mycobacterium tuberculosis* infection, including the formation of granulomas, which are aggregates of immune cells whose function may reflect success or failure of the host to contain infection. One such factor is TNF-α. TNF-α has been experimentally characterized to have the following activities in *M. tuberculosis* infection: macrophage activation, apoptosis, and chemokine and cytokine production. Availability of TNF-α within a granuloma has been proposed to play a critical role in immunity to *M. tuberculosis*. However, in vivo measurement of a TNF-α concentration gradient and activities within a granuloma are not experimentally feasible. Further, processes that control TNF-α concentration and activities in a granuloma remain unknown. We developed a multiscale computational model that includes molecular, cellular, and tissue scale events that occur during granuloma formation and maintenance in lung. We use our model to identify processes that regulate TNF-α concentration and cellular behaviors and thus influence the outcome of infection within a granuloma. Our model predicts that TNF-αR1 internalization kinetics play a critical role in infection control within a granuloma, controlling whether there is clearance of bacteria, excessive inflammation, containment of bacteria within a stable granuloma, or uncontrolled growth of bacteria. Our results suggest that there is an interplay between TNF-α and bacterial levels in a granuloma that is controlled by the combined effects of both molecular and cellular scale processes. Finally, our model elucidates processes involved in immunity to *M. tuberculosis* that may be new targets for therapy. *The Journal of Immunology*, 2011, 186: 3472–3483.

Tuberculosis (TB), a disease caused by the intracellular pathogen *Mycobacterium tuberculosis*, is responsible for 2 million to 3 million deaths per year. In the presence of an effective immune response, only 5–10% of infected people develop clinical signs of active TB (known as primary TB). However, immunological testing provides evidence of a state of latent infection, with no clinical symptoms, in one third of the world population (1). Latent TB represents a state of equilibrium in which the host controls the infection but is unable to clear it, allowing bacteria to survive at relatively constant but low levels (2). Latent infection may reactivate to active disease (reactivation TB), with an average 10% per lifetime frequency, as a result of, for example, age, impaired immunity (as in the case of HIV co-infection), malnutrition, or anti-inflammatory drug administration that interferes with host immunity (3).

The key pathological feature of TB that arises as a result of the immune response is the formation of aggregates of bacteria and immune cells within the lung called granulomas. TB granulomas, especially in humans, form as organized spherical structures composed of bacteria, a macrophage-rich core including resting, infected, and activated macrophages, and a surrounding mantle of lymphocytes. Granulomas act to immunologically restrain and physically contain *M. tuberculosis* infection (4–10). Latent and active TB in humans comprise a heterogeneous mixture of granulomas in both lung and lymph nodes that provide a range of physiological microenvironments associated with bacterial replication, persistence, and killing. Characterization of different types of granulomas will provide a framework for understanding of the immunobiology of TB that can lead to the development of new strategies for control and therapy (11, 12).

In addition to cellular components, studies in animal models and humans have identified a variety of cytokines involved in granuloma formation and function, including TNF-α and IFN-γ (reviewed in Ref. 13). These molecules are secreted from cellular sources (macrophages and T cells) as a result of *M. tuberculosis* infection, interact with receptors on target cells, trigger intracellular signaling pathways, and induce cell responses that ultimately contribute to formation of granulomas and immunologic control of *M. tuberculosis* infection (13–15). One can hypothesize that molecular scale processes that lie between the availability of particular extracellular cytokines and the final cytokine-mediated response may influence the outcome of *M. tuberculosis* infection. Receptor–ligand binding and trafficking (defined in this article to include synthesis, internalization, recycling, and degradation of the ligand and receptors) represent a group of molecular scale processes that take place under physiological conditions and are believed to play a major role in receptor-mediated cell responses (16). However, the significance of trafficking processes in controlling the

*Department of Chemical Engineering, University of Michigan, Ann Arbor, MI 48109; [†]Department of Microbiology and Immunology, University of Michigan Medical School, Ann Arbor, MI 48109; [‡]Center for Integrative Bioinformatics VU, VU University Amsterdam, Amsterdam 1081 HV, The Netherlands; and [§]Life Sciences Group, Amsterdam 1098 XG, The Netherlands

Received for publication October 7, 2010. Accepted for publication January 5, 2011.

This work was supported by National Institutes of Health Grants R33HL092844, R33HL092853, and N01 AI50018.

Address correspondence and reprint requests to Jennifer J. Linderman and Denise E. Kirschner, University of Michigan, 2300 Hayward Street, Ann Arbor, MI 48109 (J.J.L.) and University of Michigan Medical School, 6730 Medical Science Building II, 1150 W. Medical Center Drive, Ann Arbor, MI 48109 (D.E.K.). E-mail addresses: linderma@umich.edu (J.J.L.) and kirschne@umich.edu (D.E.K.)

Abbreviations used in this article: ABM, agent-based model; 2-D, two-dimensional; LHS, Latin hypercube sampling; mTNF, membrane-bound TNF-α; ODE, ordinary differential equation; PRCC, partial rank correlation coefficient; sTNF, soluble TNF-α; T_γ, proinflammatory T cells; TB, tuberculosis; TNFR1, TNF-αR1.

www.jimmunol.org/cgi/doi/10.4049/jimmunol.1003299

effect of cytokines on the host immune response (TB immune response in particular) has never been studied. Hence, a multiscale approach that considers events at the molecular, cellular, and tissue scales is required for comprehensive analysis of the role of cytokines in the complex immune response to *M. tuberculosis*.

Our study is focused on TNF-α interactions with immune cells that form a granuloma. The pleiotropic cytokine TNF-α is produced by a variety of immune cells, especially infected and activated macrophages and proinflammatory T cells (17, 18), and functions as part of the immune response to *M. tuberculosis* infection via several mechanisms. TNF-α (in conjunction with the cytokine IFN-γ) induces macrophage activation (19–21), enhances immune cell recruitment to the site of infection (22), and augments chemokine expression by macrophages through activation of the NF-κB signaling pathway (23). TNF-α can also mediate cell death via inducing the caspase-mediated apoptotic pathway (24, 25). Data identifying the roles of TNF-α include TNF-α knockout/neutralization experiments in mice and monkeys (17, 26–28), TNF-αR1 (TNFR1) knockout experiments in mice (17), and mathematical modeling studies (29, 30). Despite this wealth of information on the critical role of TNF-α in immunity to *M. tuberculosis*, many fundamental questions remain unanswered regarding the mechanisms that regulate TNF-α activity at different biological scales. For example, it is not known how the dynamics of molecular events such as TNF-α–TNFR binding and trafficking influence a granuloma's ability to control *M. tuberculosis* infection. We have recently suggested via mathematical modeling that organization of immune cells as well as the processes of TNF-α–TNFR binding and trafficking control steady-state TNF-α availability within an existing granuloma. This results from a TNF-α concentration gradient that is created with the highest concentration at the core of granuloma (31). However, important unanswered questions remain: What factors control such a gradient during a long-term immune response to *M. tuberculosis* infection that includes formation and maintenance of granulomas? How does this gradient regulate TNF-α–associated processes and ultimately translate to the outcome of *M. tuberculosis* infection? Is there an interplay between TNF-α availability and bacterial load in a granuloma? Are there TNF-α–level processes that, if targeted, could present new strategies for disease therapy?

These questions invoke multiple biological scales (in length and time) that are currently difficult to address experimentally. Hence, a systems biology approach that incorporates computational modeling to generate and test hypotheses, run virtual experiments, and make experimentally testable predictions is uniquely suited to address these questions. We develop a multiscale computational model that describes the immune response to *M. tuberculosis* in the lung over three biological length scales: molecular, cellular, and tissue. We use the model to track formation and maintenance of a granuloma in space and time. The model captures the dynamics of TNF-α–TNFR interactions that occur on the second to minute timescales within the long-term immune response to *M. tuberculosis* infection, a complex process that lasts for months to years. We identify TNF-α–associated processes that influence infection outcome at the granuloma scale as well as predict cellular scale processes that influence TNF-α availability. Finally, we identify processes that regulate TNF-α concentration and cellular behaviors and thus influence the outcome of infection within a granuloma.

Materials and Methods

An overview of the multiscale granuloma model

To build a multiscale model necessary to address the questions regarding TNF-α–regulated immune responses to *M. tuberculosis* infection in the lung, we need to first have working models at both the cellular/tissue scale and the molecular/single-cell scale. We briefly describe these models below and then describe our approach for linking them. Cellular and tissue scale dynamics are captured via a set of well-described interactions between immune cells and *M. tuberculosis* at the site of infection using stochastic simulations in the form of an agent-based model (ABM). Single-cell molecular scale processes that control TNF-α–TNFR binding and trafficking for each individual cell are captured by a set of nonlinear ordinary differential equations (ODEs). Fig. 1 indicates how these models exist separately and how they are linked into a single multiscale granuloma model. The linkage is achieved via TNF-α–induced cell responses (i.e., apoptosis and NF-κB activation) that are modeled as Poisson processes with rate parameters computed as functions of molecular concentrations from the ODE model. Further details of the rules, equations, and parameters of the multiscale model are described in this article and in the online supporting text, tables, and videos at http://malthus.micro.med.umich.edu/lab/movies/Multiscale/GranSim/.

Cellular/tissue scale model

The two-dimensional (2-D) ABM used in this study is an updated version of our previous model that captures cellular scale interactions leading to a tissue-level readout, namely granuloma formation in response to *M. tuberculosis* infection in primates (30). Because multiscale analysis of the long-term immune response to *M. tuberculosis* is the aim of this study, an extensive sensitivity analysis is required. Therefore, choosing a 2-D model that can be used to run a large number of simulations in a reasonable time frame is key for our study. A comparison with a simple three-dimensional version has shown that our 2-D model can capture important dynamics of *M. tuberculosis* infection (32). Fig. 1*A* depicts a schematic overview of selected immunological interactions tracked at the cellular scale. A full description of all ABM rules that reflect known biological activities is provided in the online supporting text at http://malthus.micro.med.umich.edu/lab/movies/Multiscale/GranSim/, and significant updates to the original model are highlighted. Briefly, rule events include chemotactic movement and recruitment of immune cells to site of infection, intracellular and extracellular growth of *M. tuberculosis*, phagocytosis of bacteria by macrophages, cell death and apoptosis, macrophage–T cell interactions such as cytolytic functions of cytotoxic T cells and IFN-γ based activation of macrophages by proinflammatory T cells (Tγ), downregulation of immune cells by regulatory T cells, secretion of chemokines, and caseation.

One important simplification in our model is the choice to include only cell types with well-characterized roles in *M. tuberculosis* granulomas (macrophages, cytotoxic T cells, Tγ, and T regulatory cells). Cell types that may have important roles but are not sufficiently characterized at this point to include in mechanistic ways in the model include neutrophils [with protective roles in early infection that may be immunomodulatory in nature (33–35)], multinucleate giant cells [may modulate chemokine production (36, 37)], dendritic cells [for optimal antigenic stimulation of T cells (38, 39)], and foamy cells [possible nutrient source for bacteria (40, 41)]. Future work can easily incorporate them into the model when more mechanistic data become available.

Molecular/single-cell scale TNF-α–TNFR model

The kinetic processes of TNF-α–TNFR binding and trafficking (synthesis, internalization, recycling, and degradation of ligand and receptors) occurring in individual cells within a granuloma can be described by ODEs (31). As schematically shown in Fig. 1*B*, TNF-α is first synthesized by TNF-α–producing cells, including infected macrophages, chronically infected macrophages, NF-κB–activated resting macrophages, activated macrophages and T cells, as a membrane-bound precursor form (mTNF) that can then be processed and released as a soluble form (sTNF) into extracellular spaces. Two types of TNFR (TNFR1 and TNFR2) are synthesized and expressed on the cell membrane. The equations describing TNF-α–TNFR processes for an individual cell are detailed in the online supporting text and Tables S3 and S4 at http://malthus.micro.med.umich.edu/lab/movies/Multiscale/GranSim/.

Linking the individual models via sTNF-induced cell responses

Activation of the two major TNF-α–induced signaling pathways, the caspase-mediated apoptotic pathway and the NF-κB pathway, are both controlled at the level of sTNF–TNFR1 interactions and thus serve as the link between the molecular/single-cell scale TNF-α–TNFR kinetic model and the cellular/tissue scale model. The NF-κB signaling pathway is initiated by sTNF-bound cell surface TNFR1, and apoptosis depends on the internalized sTNF–TNFR1 complexes (42–44). As reported in the literature, NF-κB activation of macrophages is a necessary but not sufficient factor in successful immune response to mycobacterial infection. Its role

includes induction of a variety of inflammatory-related genes such as TNF-α and chemokines as well as controlling phagolysosome fusion-mediated killing of mycobacteria by activated macrophages (20, 45). TNF-α–induced apoptosis of macrophages kills intracellular bacteria and is associated with a better outcome of infection (3). In addition to sTNF, mTNF has also been shown to contribute in part to control of *M. tuberculosis* infection in mice (46–48). However, experimental data regarding molecular and cellular-level details of mTNF-mediated signaling and reverse signaling in *M. tuberculosis* immune responses are limited. Thus, at this time we only consider in our model signaling mediated by sTNF–TNFR1.

A recent study has shown that TNF-α–induced NF-κB activation is a process with a discrete nature at the single-cell level, with fewer cells responding at lower doses (49). Accordingly, we describe TNF-α–induced NF-κB activation for each individual macrophage as a Poisson process with a probability determined within each time-step (Δt), based on a Poisson rate parameter that is a function of the NF-κB activation rate constant ($k_{\text{NF-κB}}$), the concentration of cell surface sTNF–TNFR1 complexes [sTNF–TNFR1], and the concentration threshold for cell surface sTNF–TNFR1 ($\tau_{\text{NF-κB}}$):

$$P_{\text{NF-κB}} = \begin{cases} 0 & ; [\text{sTNF}-\text{TNFR1}] < \tau_{\text{NF-κB}} \\ 1 - e^{-k_{\text{NF-κB}}([\text{sTNF-TNFR1}] - \tau_{\text{NF-κB}})\Delta t} & ; [\text{sTNF}-\text{TNFR1}] \geq \tau_{\text{NF-κB}}. \end{cases} \quad (1)$$

Similarly, we model TNF-α–induced apoptosis for each individual cell (macrophage and T cell) by:

$$P_{\text{apopt}} = \begin{cases} 0 & ; [\text{sTNF}-\text{TNFR1}_{\text{i}}] < \tau_{\text{apopt}} \\ 1 - e^{-k_{\text{apopt}}([\text{sTNF-TNFR1}_{\text{i}}] - \tau_{\text{apopt}})\Delta t} & ; [\text{sTNF}-\text{TNFR1}_{\text{i}}] \geq \tau_{\text{apopt}}. \end{cases} \quad (2)$$

We use a Poisson process with a probability computed as a function of the apoptosis rate constant (k_{apopt}), the concentration of internalized sTNF–TNFR1 complexes [sTNF–TNFR1$_{\text{i}}$], and the concentration threshold for internalized sTNF–TNFR1 (τ_{apopt}). Scale-linking parameters, or simply "linking parameters", that is, TNF-α–response parameters (defined to include parameters introduced in Equations 1 and 2), are listed in Table S5 at http://malthus.micro.med.umich.edu/lab/movies/Multiscale/GranSim/.

To analyze how TNF-α affects infected versus resting macrophages in a granuloma, we define infected/resting cell ratios, $R_{\text{apoptosis}}$ and $R_{\text{NF-κB}}$, as follows. $R_{\text{apoptosis}}$ is defined as the ratio of the number of infected macrophages that undergo TNF-α–mediated apoptosis to the number of resting macrophages that undergo TNF-α–mediated apoptosis during a 200-d period postinfection. $R_{\text{NF-κB}}$ is similarly defined as the number of infected macrophages that undergo TNF-α–mediated NF-κB activation to the number of resting macrophages that undergo TNF-α–mediated NF-κB activation during a 200-d period postinfection.

Parameter estimation and control experiments

We estimate ABM parameter values from literature data as described in detail by Ray et al. (30). When data are not available, we use uncertainty analysis to explore the entire parameter space of possible model outcomes as described in Ref. 50. Cell-specific TNFR densities and rate constants for TNF-α–TNFR processes are estimated based on experimental data from our group (31) and other groups as indicated in Table S2 at http://malthus.micro.med.umich.edu/lab/movies/Multiscale/GranSim/. Values of parameters used to describe TNF-α–induced cell responses, including NF-κB activation and apoptosis (i.e., linking parameters), are estimated via uncertainty analysis by varying parameter values in ranges that are qualitatively consistent with experimental and modeling data on timescales and thresholds for TNF-α–induced cell responses (49, 51, 52).

Using the above methods, we specify a baseline set of parameter values that robustly leads to control of infection in granulomas with organized structures as reported for humans and nonhuman primates (Tables S1, S2, and S5 at http://malthus.micro.med.umich.edu/lab/movies/Multiscale/GranSim/). We then explore parameter changes that shift infection outcome to clearance or uncontrolled growth of *M. tuberculosis*. To test further the ability of the model to predict different infection outcomes under pathological conditions compatible with both experimental and previous modeling data on granuloma formation, we simulate gene knockouts of previously identified essential components of the *M. tuberculosis* immune response (e.g., TNF-α, IFN-γ, and T cell knockouts). To do this, we set relevant probabilities or rate constants to zero from the beginning of simulations.

Sensitivity analysis

When computational models include parameters describing a large number of known biological processes, it is critical to understand the role that each of these parameters plays in determining output. Sensitivity analysis is a technique to identify critical parameters of a model and quantify how input uncertainty impacts model outputs. Latin hypercube sampling (LHS) is an algorithm that allows multiple parameters to be varied and sampled simultaneously in a computationally efficient manner (53). We use LHS sensitivity analysis as described for application to ABMs (50) to analyze the impact of TNF-α–TNFR trafficking and TNF-α response (linking) parameter values as well as TNF-α–independent and cellular scale parameter values (as listed in Tables S1, S2, and S5 at http://malthus.micro.med.umich.edu/lab/movies/Multiscale/GranSim/) on model outputs. For clarity, these outputs are grouped, as TNF-α function-related outputs (total number of TNF-α–induced events, including NF-κB activation and apoptosis in different types of cells), cellular-level outputs (total bacteria, macrophage, and T cell numbers), tissue-level outputs (granuloma size and caseation area), and average tissue concentrations of TNF-α and chemokines. The correlation of model outputs with each parameter is quantified via calculation of a partial rank correlation coefficient (PRCC). PRCC values vary between −1 (perfect negative correlation) and +1 (perfect positive correlation) and can be differentiated based on p values derived from Student t test. LHS simulations sampled each parameter 250 times. Each sampled parameter set was run four times, and averages of the outputs were used to calculate PRCC values. The choice of the number of simulations is determined by the desired significance level for the PRCC (50, 53). In this study, 250 runs imply that PRCC values above +0.24 or below −0.24 are significantly different from zero ($p < 0.001$). To study how processes at different scales interact with each other, we analyze the effect of parameters associated with each scale on the outputs of the same scale (intrascale sensitivity analysis) as well as on the outputs of the other scale (interscale sensitivity analysis).

Computer simulations and visualization

The model was implemented in C++. We use Qt, a C++ framework for developing cross-platform applications with a graphical user interface, to visualize and track different aspects of the granuloma, including the structure and molecular concentration gradients, as it forms and is maintained. Simulations can be run with or without graphical visualization. Simulations were run on Linux and Mac operating systems.

Results

Prediction of different infection outcomes at the granuloma level

We first tested whether our multiscale computational model (Fig. 1) could capture key features of granuloma formation and maintenance. Using a combination of parameter estimation and uncertainty analysis as described in *Materials and Methods*, we identified a set of baseline values for model parameters, including cellular/tissue scale parameters (Table S1 at http://malthus.micro.med.umich.edu/lab/movies/Multiscale/GranSim/), molecular/single-cell scale TNF-α–TNFR parameters (Table S2 at http://malthus.micro.med.umich.edu/lab/movies/Multiscale/GranSim/), and parameters that link the two scales in the model (Table S5 at http://malthus.micro.med.umich.edu/lab/movies/Multiscale/GranSim/). This set of parameter values leads to containment: control of *M. tuberculosis* infection within a well-circumscribed granuloma containing stable bacterial levels ($<10^3$ total bacteria) at 200 d postinfection (Fig. 2*A*, 2*B*) (see Video 1 at http://malthus.micro.med.umich.edu/lab/movies/Multiscale/GranSim/). This recapitulates a state that has been described as an equilibrium between the host and *M. tuberculosis* at the level of single granuloma and is referred to as a solid granuloma with caseous center (*M. tuberculosis* containment) (3, 54). As observed in Video 1 at http://malthus.micro.med.umich.edu/lab/movies/Multiscale/GranSim/, simulated granulomas form as organized immune structures predominately composed of uninfected macrophages surrounding a core of bacteria and infected and activated macrophages with T cells localized at the periphery (4–10). As reported for most animal models of TB, bacterial growth increases logarithmically until reaching a plateau coincident with T cell response initiation (55).

As observed in nonhuman primate models as well as in humans, several types of granuloma are observed in *M. tuberculosis* infection (56). Our multiscale model is also able to recapitulate

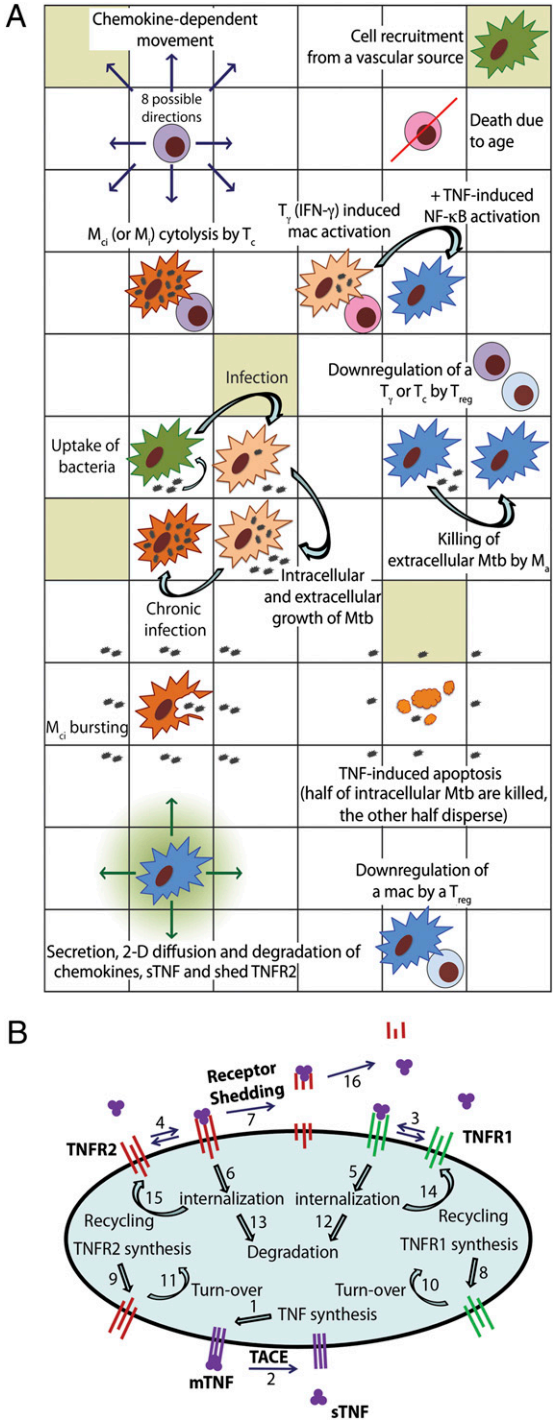

FIGURE 1. Schematic representation of the multiscale model of the immune response to *M. tuberculosis* infection in the lung. *A*, An overview of selected cell-level ABM rules based on known immunological activities and interactions. *B*, Schematic representation of binding interactions and reactions controlling TNF-α–TNFR dynamics at the single-cell level with numbers that represent model processes as listed in Table S3 at http://malthus.micro.med.umich.edu/lab/movies/Multiscale/GranSim/.

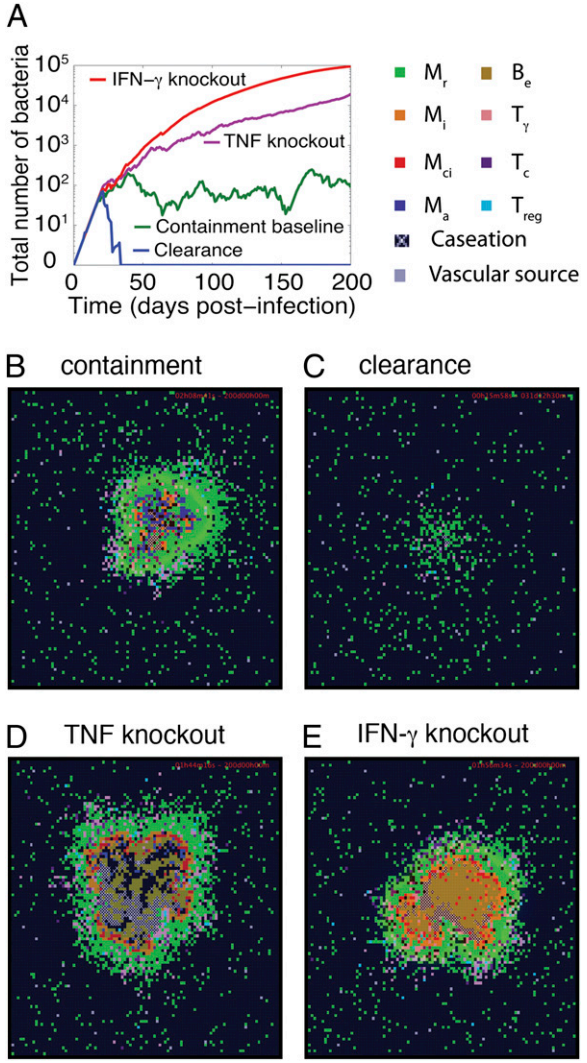

FIGURE 2. Simulation results for the *M. tuberculosis* dynamics and granuloma structures at 200 d postinfection under different pathological conditions. *A*, Changes of total number of *M. tuberculosis* (intracellular and extracellular bacteria, i.e., $B_{int} + B_{ext}$) with time for simulation of containment baseline, a scenario of *M. tuberculosis* clearance, a TNF-α (or TNFR1) knockout scenario, and an IFN-γ knockout scenario. *B–E*, Granuloma snapshots for (*B*) a scenario of containment, (*C*) clearance of *M. tuberculosis* infection in less than 5 wk as a result of an efficient immune response, (*D*) a TNF-α (or TNFR1) knockout scenario, and (*E*) an IFN-γ knockout scenario. Cell types and status are defined by different colors, as indicated in the *upper right corner* of the figure. Caseation and vascular sources are also indicated. B_e, extracellular bacteria; M_a, activated macrophage; M_{ci}, chronically infected macrophage; M_i, infected macrophage; M_r, resting macrophage; T_γ, proinflammatory IFN-γ producing T cell; T_c, cytotoxic T cell; T_{reg}, regulatory T cell).

different granuloma types with different abilities to control infection as we vary specific parameters identified as important via sensitivity analysis from their baseline values (see Tables S1, S2, and S5 at http://malthus.micro.med.umich.edu/lab/movies/Multiscale/GranSim/). Cellular scale processes identified to control significantly bacterial numbers, caseation, and granuloma size at 200 d postinfection are bacterial growth, T_γ cell-induced STAT1 activation of macrophages, and T cell movement and recruitment (T_γ cells in particular). These results are highlighted in Table I and are consistent with available experimental data reviewed in Refs. 3, 57, and 58 and our previous modeling studies (30, 59). Greater intracellular *M. tuberculosis* growth rates, in agreement with published data (60), lead to higher bacterial loads and larger granulomas with larger caseation areas. STAT1 activation of macrophages by IFN-γ–producing T_γ cells is required for activation of macrophages and killing of intracellular and extracellular *M. tuberculosis*. Recruitment of IFN-γ–producing T_γ cells to site of infection is a critical component of immunity to *M. tuberculosis* as a smaller TNF-α/chemokine concentration threshold for T_γ cell recruitment leads to more effi-

Table I. Model parameters significantly correlated with outputs of interest, bacterial numbers, granuloma size, caseation area, and TNF-α concentration at day 200 postinfection

Selected Model Outputs	Important TNF-α–Independent and Cellular Scale Parameters [a,b]	Important TNF-α–TNFR-Associated Molecular and Linking Parameters [a,c]
Total number of bacteria	α_{Bi} (++)	$k_{synthMac}$ (−−)
	P_{STAT1} (−−)	δ_{TNF} (++)
	T_{moveM} (−−)	K_{d1} (+)
	T_{recr} (−−)	k_{int1} (+)
	$\tau_{recTgam}$ (++)	$TNFR1_{mac}$ (−)
	D_{chem} (−−)	$k_{NF\text{-}\kappa B}$ (−−)
	δ_{chem} (++)	$\tau_{NF\text{-}\kappa B}$ (++)
Granuloma size	α_{Bi} (++)	$k_{synthMac}$ (−−)
	P_{STAT1} (−)	δ_{TNF} (++)
	M_{recr} (++)	K_{d1} (++)
	T_{moveM} (−−)	k_{int1} (+)
	T_{recr} (−−)	$TNFR1_{mac}$ (−−)
	$P_{apop/Fas}$ (−)	$k_{NF\text{-}\kappa B}$ (−−)
	$\tau_{recTgam}$ (++)	$\tau_{NF\text{-}\kappa B}$ (++)
Caseation	α_{Bi} (++)	$k_{synthMac}$ (−−)
	P_{STAT1} (−)	δ_{TNF} (++)
	M_{recr} (++)	K_{d1} (++)
	T_{moveM} (−−)	k_{int1} (+)
	T_{recr} (−−)	k_{rec1} (++)
	$\tau_{recTgam}$ (++)	$TNFR1_{mac}$ (−−)
	δ_{chem} (++)	k_{apopt} (−)
	τ_{chem} (+)	$k_{NF\text{-}\kappa B}$ (−−)
		$\tau_{NF\text{-}\kappa B}$ (++)
Average tissue concentration of sTNF	α_{Bi} (++)	$k_{synthMac}$ (−−)
	P_{STAT1} (−)	K_{d1} (+)
	T_{moveM} (−−)	$TNFR1_{mac}$ (−)
	T_{recr} (−−)	$k_{NF\text{-}\kappa B}$ (−−)
	$\tau_{recTgam}$ (++)	$\tau_{NF\text{-}\kappa B}$ (+)
	δ_{chem} (++)	
	τ_{chem} (+)	

[a]Only parameters with significant PRCC values are indicated. Significant positive and negative correlations are shown using + and − as follows: −/+: $0.001 < p < 0.01$.−−/++: $p < 0.001$.

[b]TNF-α–independent and cellular scale parameter descriptions are as follows: α_{Bi}, intracellular *M. tuberculosis* growth rate; P_{STAT1}, probability of STAT-1 activation in M_r or M_i; T_{moveM}, probability of T cell moving to a macrophage-containing location; T_{recr}, probability of T cell recruitment; M_{recr}, probability of M_r recruitment; $\tau_{recTgam}$, TNF-α/chemokine concentration threshold for T_γ cell recruitment; $P_{apop/Fas}$, probability of Fas/FasL apoptosis by T_γ cell; D_{chem}, diffusion coefficient of chemokines; δ_{chem}, chemokine degradation rate constant; τ_{chem}, minimum chemokine concentration detection threshold.

[c]TNF-α–TNFR-associated parameter descriptions are as follows: $k_{synthMac}$, mTNF synthesis rate for macrophages; δ_{TNF}, sTNF degradation rate constant; K_{d1}, equilibrium dissociation constant of sTNF–TNFR1; k_{int1}, TNFR1 internalization rate constant; k_{rec1}, TNFR1 recycling rate constant; $TNFR1_{mac}$, TNFR1 density on the surface of macrophages; k_{apopt}, rate constant for TNF-α–induced apoptosis in all cell types; $k_{NF\text{-}\kappa B}$, rate constant for TNF-α–induced NF-κB activation in macrophages; $\tau_{NF\text{-}\kappa B}$, cell surface sTNF–TNFR1 threshold for TNF-α–induced NF-κB activation.

Detailed sensitivity analysis results are presented in Tables S6 and S7 at http://malthus.micro.med.umich.edu/lab/movies/Multiscale/GranSim/.

cient responses. Further, the ability of T cells to migrate through a dense uninfected macrophage network surrounding bacteria and infected macrophages at the core of a granuloma helps determine the efficiency of the T cell-mediated immune response to *M. tuberculosis*.

In addition to containment, we can reproduce other possible outcomes of *M. tuberculosis* infection, including clearance and uncontrolled growth of bacteria, by manipulating values of important model parameters. For example, an increase in the ability of T cells to penetrate into the site of infection at the core of granuloma by increasing the value of model parameter T_{move}, the probability of a T cell moving onto a macrophage-containing microcompartment, significantly increases the efficiency of the T cell-mediated response and thus favors *M. tuberculosis* clearance (Fig. 2*A*, 2*C*) (see Video 2 at http://malthus.micro.med.umich.edu/lab/movies/Multiscale/GranSim/). In contrast, simulations of gene knockouts of essential components of the *M. tuberculosis* immune response such as TNF-α or TNFR1 knockouts ($k_{synthMac} = k_{synthTcell} = 0$ or $TNFR1_{mac} = TNFR1_{Tcell} = 0$) and IFN-γ knockout ($P_{STAT1} = 0$) lead to uncontrolled growth of *M. tuberculosis*. This is consistent with a variety of data on the crucial role of these cytokines in immunity to *M. tuberculosis* (3, 13, 61). In this case, granulomas that form are greater in size, irregular in structure, and include very high numbers of extracellular *M. tuberculosis*, large numbers of infected macrophages, and widespread caseation (dead tissue caused by multiple deaths of macrophages in tissue usually within the core of the granuloma) (Fig. 2*A*, 2*D*, 2*E*) (see Videos 3 and 4 at http://malthus.micro.med.umich.edu/lab/movies/Multiscale/GranSim/). Overall, our multiscale model, which includes molecular (TNF-α–associated), cellular, and tissue scale events, predicts dynamics of *M. tuberculosis* infection for different infection scenarios, including containment, clearance, and uncontrolled growth of bacteria as well as a variety of structural and functional outcomes that are expected to occur under different pathological conditions. Our results for these conditions are in agreement with our previous study using a model without molecular (TNF-α–associated) events (30) and a variety of experimental data. We now turn our analysis to the important role that TNF-α plays and the factors that affect the ability of TNF-α to play that role during the immune response to *M. tuberculosis*.

Cellular scale processes control TNF-α concentration by affecting bacterial load

We know from experimental studies that artificial manipulation of TNF-α concentration via anti–TNF-α treatments negatively affects infection outcome in mice, humans, and nonhuman primates (26, 27, 62, 63). Are there physiological processes within the granuloma that also affect TNF-α concentration, and does alteration of those processes similarly affect infection outcome? To answer this question, we used sensitivity analysis to identify critical TNF-α–independent and cellular scale parameters that influence TNF-α concentration. Notably, processes highlighted in the previous section to be important determinants of bacterial numbers, caseation, and granuloma size also significantly impact TNF-α concentration and thus the number of TNF-α–induced NF-κB activation and apoptosis events (Table I; Table S6 at http://malthus.micro.med.umich.edu/lab/movies/Multiscale/GranSim/). This is because TNF-α production within the granuloma strongly depends on the level of infection. For example, reducing the probability of T cell recruitment (T_{recr}) decreases the level of T cell-mediated macrophage activation, a process that is necessary for limiting *M. tuberculosis* growth in infected macrophages. Therefore, intracellular *M. tuberculosis* can grow, disperse in the tissue after bursting of chronically infected macrophages, and infect more resting macrophages. This ultimately increases the number of extracellular *M. tuberculosis* as well as the number of infected macrophages that act as further TNF-α sources in the tissue. TNF-α also enhances activation and recruitment of immune cells, leading to larger granulomas. This is in agreement with data from animal models that show increased bacterial numbers result in increased inflammation and more immune cell recruitment (64).

TNF-α–TNFR molecular processes control TNF-α actions and thus ability of a granuloma to control infection

The analysis above indicates that physiological processes that affect bacterial load indirectly affect TNF-α concentration. Are there other processes that more directly act on TNF-α, and would manipulation of those processes alter infection outcome? To answer this question, we performed sensitivity analysis to identify

molecular scale and linking parameters associated with TNF-α–TNFR that influence model outcomes. Both signaling and trafficking processes are identified to significantly influence granuloma function, as indicated in Table I and in Table S7, which can be found at http://malthus.micro.med.umich.edu/lab/movies/Multiscale/GranSim/. TNF-α–induced NF-κB activation of resting and infected macrophages strongly correlates with bacterial numbers. Increasing the rate constant for TNF-α–induced NF-κB activation or reducing its cell surface sTNF–TNFR1 concentration threshold leads to faster macrophage NF-κB activation responses by smaller concentrations of available sTNF. Thus, these parameters can significantly influence the outcome of infection. This is consistent with the published data on the role of NF-κB activation of macrophages in killing mycobacteria (20).

Receptor and ligand trafficking processes that strongly influence infection outcome are mTNF synthesis by infected and activated macrophages, sTNF degradation, TNFR1 affinity for sTNF, TNFR1 density on the membrane of macrophages, and sTNF-induced internalization of TNFR1 (Table I; Table S7 at http://malthus.micro.med.umich.edu/lab/movies/Multiscale/GranSim/). The rate of mTNF synthesis by infected and activated macrophages positively correlates with two key TNF-α functions (NF-κB activation and apoptosis) and negatively correlates with bacterial load, numbers of infected and chronically infected macrophages, as well as granuloma and caseation size. This is consistent with human and animal model data and our previous studies on the crucial role of TNF-α in controlling *M. tuberculosis* infection (26, 29, 30, 62, 65). Similarly, the rate of sTNF degradation negatively influences TNF-α activities and thus positively correlates with bacterial numbers within a granuloma. TNFR1 density on macrophage membranes has a negative impact on bacterial numbers. This is consistent with experimental data on the importance of TNFR1 in controlling *M. tuberculosis* infection (17). A greater TNFR1 affinity for binding to sTNF (smaller K_{d1}) also enhances the level of TNF-α–induced NF-κB activation and apoptosis and reduces total bacterial numbers. Internalization of TNFR1 occurs as a result of sTNF binding to TNFR1 on cell membranes and not only is required for TNF-α–induced apoptosis (42–44) but also reduces sTNF in a granuloma (31). Thus, TNFR1 internalization enhances apoptosis in TNF-α–secreting infected macrophages but reduces levels of NF-κB activation in non–TNF-α–secreting resting macrophages by limiting TNF-α concentrations near these cells (Table S7 at http://malthus.micro.med.umich.edu/lab/movies/Multiscale/GranSim/). Overall, our sensitivity analysis predicts that sTNF-induced TNFR1 internalization increases bacterial levels within a granuloma. We focus our next analysis on potential effects of manipulation in TNFR1 internalization.

TNF-α–TNFR trafficking dynamics balance inflammation and bacterial killing

The effect of changing the rate constant for TNFR1 internalization on sTNF concentration, recruitment of immune cells, macrophage activation, and apoptosis is shown in Fig. 3. As described above, sTNF-induced TNFR1 internalization, the key process in TNF-α–TNFR trafficking, has a significant impact on responses at molecular, cellular, and tissue scales. The value of the rate constant for TNFR1 internalization (k_{int1}) controls sTNF concentration dynamics during the immune response to *M. tuberculosis* (Fig. 3*A*). The physiological rate of TNFR1 internalization [half-time of ~15 min (66, 67), $k_{int1} = 7.7 \times 10^{-4}\ s^{-1}$] leads to much less extracellular sTNF in the tissue compared with that in the scenario in which sTNF–TNFR1 complex on the cell membrane is not at all ($k_{int1} = 0$) or is very slowly internalized (half-time of ~115 min, $k_{int1} = 1.0 \times 10^{-4}\ s^{-1}$) (Fig. 3*B*). Although TNF-α is required for control of *M. tuberculosis* infection and the protective granulomatous response, high concentrations of TNF-α may lead to excessive inflammation and cause immunopathology (61, 68). Therefore, we predict that TNF-α–TNFR trafficking plays an important role in preventing excessive inflammation. Indeed, the rate of sTNF-induced internalization of TNFR1 controls the concentration of available TNF-α in tissue and regulates cell infiltration by affecting the extent and dynamics of TNF-α–dependent recruitment and activation of immune cells as well as mediating TNF-α–induced apoptosis (Fig. 3*C*–3*F*). Thus, a hyperinflammatory state may occur in the absence of a sufficiently rapid sTNF-induced TNFR1 internalization, leading to early and extensive recruitment of macrophages and T cells as well as uncontrolled activation of a large fraction of macrophages that are unable to undergo apoptosis efficiently. Notably, increasing TNFR1 internalization rate constant to $k_{int1} = 1.5 \times 10^{-3}\ s^{-1}$ (corresponding with a half-time of ~7.7 min) does not have a large effect on either sTNF concentration or immune cell population dynamics but does significantly enhance the number of apoptotic macrophages. However, further analysis reveals that other model outputs may be significantly affected by increasing TNFR1 internalization rate constant.

In addition to an impact on inflammation, TNF-α–TNFR trafficking dynamics are capable of exerting a dramatic effect on the bacterial outcome of *M. tuberculosis* infection in a granuloma (Fig. 4). Zero to slow rates of sTNF-induced TNFR1 internalization (half-time of ≥23 min, $k_{int1} \leq 5.0 \times 10^{-4}\ s^{-1}$) favor clearance of bacteria, a moderate (physiological) rate (half-time of ~15 min, $k_{int1} = 7.7 \times 10^{-4}\ s^{-1}$) leads to containment of bacteria, and a rapid rate of TNFR1 internalization (half-time of ~7.7 min, $k_{int1} = 1.5 \times 10^{-3}\ s^{-1}$) results in uncontrolled growth of *M. tuberculosis* within the 200-d period of infection (Fig. 4) (see Videos 5–8 at http://malthus.micro.med.umich.edu/lab/movies/Multiscale/GranSim/). However, zero or very slow rates of TNFR1 internalization (e.g., half-time of ~115 min, $k_{int1} = 1.0 \times 10^{-4}\ s^{-1}$) result in clearance of infection at the expense of extensive inflammation. Thus, our model suggests that there may exist an optimum rate of sTNF-induced TNFR1 internalization that balances the impacts that TNF-α has on control of *M. tuberculosis* infection and inflammation in tissue. We now investigate mechanisms underlying this balance.

Do high rates of TNFR1 internalization and slow rates of TNF-α synthesis have the same effects?

In the previous section, we showed that the rate of sTNF-induced TNFR1 internalization significantly affects the immune response to *M. tuberculosis*; a small value of TNFR1 internalization rate constant favors *M. tuberculosis* clearance, and increasing the rate of TNFR1 internalization leads to uncontrolled growth of *M. tuberculosis*. One might argue that such an effect is simply attributable to the role of TNFR1 internalization in reducing sTNF concentration in the granuloma and that therefore an increase or a decrease in the rate of TNF-α synthesis may compensate for the effects of increasing or decreasing the rate of TNFR1 internalization. To test this hypothesis, we compare the effects of manipulating rates of TNFR1 internalization and mTNF synthesis by macrophages on model outputs (such as bacterial numbers and inflammation). As indicated in Fig. 5*A*, a zero rate of TNFR1 internalization and a high rate of TNF-α synthesis both result in *M. tuberculosis* clearance. However, high rates of TNF-α synthesis, in contrast to very slow or zero rates of TNFR1 internalization, do not lead to dramatic increases in sTNF concentration and macrophage activation (Fig. 5*B*, 5*C*). This is because impairing TNFR1 internalization has a negative effect on rates of TNF-α–induced apoptosis (Fig. 5*D*), a process that has been suggested to be important for controlling the level of inflammation

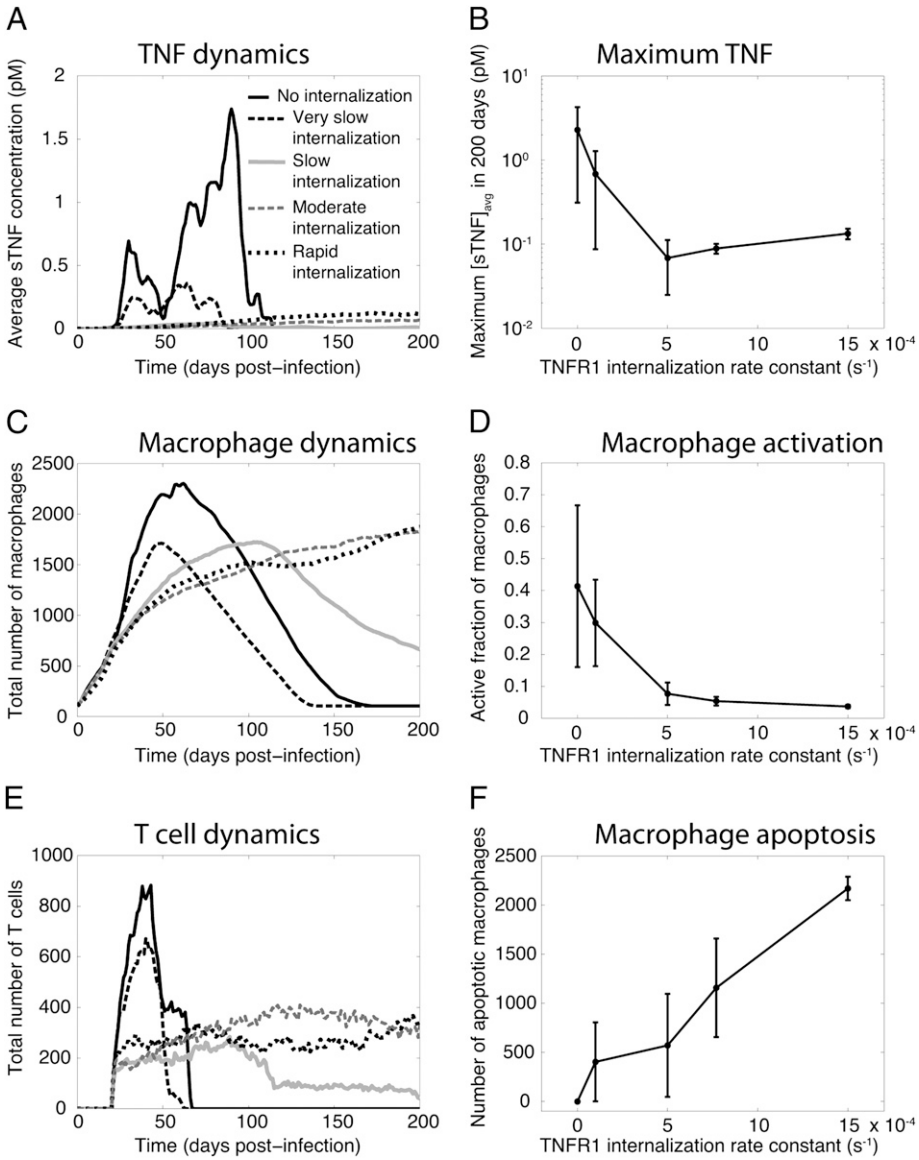

FIGURE 3. TNFR1 internalization dynamics control sTNF concentration as well as macrophage and T cell recruitment and behavior. Simulation results show (*A*) sTNF concentration dynamics, (*B*) maximum simulated sTNF concentration as a function of TNFR1 internalization rate constant (k_{int1}), (*C*) macrophage recruitment dynamics, (*D*) maximum fraction of macrophages that become activated after *M. tuberculosis* infection, (*E*) T cell recruitment dynamics, (*F*) TNF-α–induced macrophage apoptosis within a 200-d period after *M. tuberculosis* infection. No internalization, $k_{int1} = 0$; very slow internalization, $k_{int1} = 1.0 \times 10^{-4}$ s^{-1}; slow internalization, $k_{int1} = 5.0 \times 10^{-4}$ s^{-1}; moderate internalization, $k_{int1} = 7.7 \times 10^{-4}$ s^{-1}; and rapid internalization, $k_{int1} = 1.5 \times 10^{-3}$ s^{-1}.

(30). However, high rates of TNF-α synthesis favor apoptosis of macrophages and thus do not lead to extensive inflammation.

In contrast, a rapid rate of TNFR1 internalization and a small rate of TNF-α synthesis both result in uncontrolled growth of *M. tuberculosis*, although to different extents (Fig. 5*A*). This difference can be explained by high levels of TNF-α–induced apoptosis in macrophages (and thus infected macrophages) for high values of TNFR1 internalization rate constant, whereas a small rate of TNF-α synthesis leads to lower levels of apoptosis (Fig. 5*D*). Apoptosis of infected macrophages can help with reducing intracellular bacterial burden (25). Thus, our results suggest that the impact of TNF-α–TNFR trafficking on *M. tuberculosis* infection is more complex than simply changing the TNF-α concentration in the granuloma.

TNFR1 internalization controls the spatial range of TNF-α action within a granuloma

As demonstrated earlier, sTNF-induced TNFR1 internalization controls both *M. tuberculosis* infection and inflammation in tissue. How does this process play such a key role? We explored the possibility that the spatial range of TNF-α action underlies the important effects of the rate of TNFR1 internalization on granuloma function. By spatial range of TNF-α action, we mean the area surrounding the center of granuloma, as indicated in Fig. 6*A*, within which macrophages become activated or undergo apoptosis via autocrine or paracrine stimulation pathways (19, 25, 69). As infected macrophages are located in the core of granuloma surrounded by resting macrophages, the spatial range of TNF-α action is correlated with the infection status of macrophages affected by TNF-α. Thus, motivated by our sensitivity analysis (Table S7 at http://malthus.micro.med.umich.edu/lab/movies/Multiscale/GranSim/), we explored the possibility that TNF-α–TNFR trafficking leads to differential effects on TNF-α–mediated responses in cells of different infection status. We analyzed the infection status of macrophages affected by TNF-α–induced events (either NF-κB activation or apoptosis) after *M. tuberculosis* infection by computing infected/resting cell ratios, $R_{NF\text{-}\kappa B}$ and $R_{apoptosis}$, as defined in *Materials and Methods* (Fig. 6*B*). These ratios compare TNF-α effects on infected macrophages versus resting macrophages during the *M. tuberculosis* immune response. Our model predicts a very significant effect of TNFR1 internalization on both $R_{apoptosis}$ and $R_{NF\text{-}\kappa B}$ (Fig. 6*B*). At very slow rates of sTNF-induced TNFR1 internalization (half-time of ~115 min, $k_{int1} = 1.0 \times 10^{-4}$ s^{-1}), resting macrophages are the main cells affected by both TNF-α–mediated apoptosis and NF-κB signaling pathways ($R_{apoptosis}$ and $R_{NF\text{-}\kappa B} << 1$). However, with a dramatic increase in the rate of TNFR1 internalization (to a half-

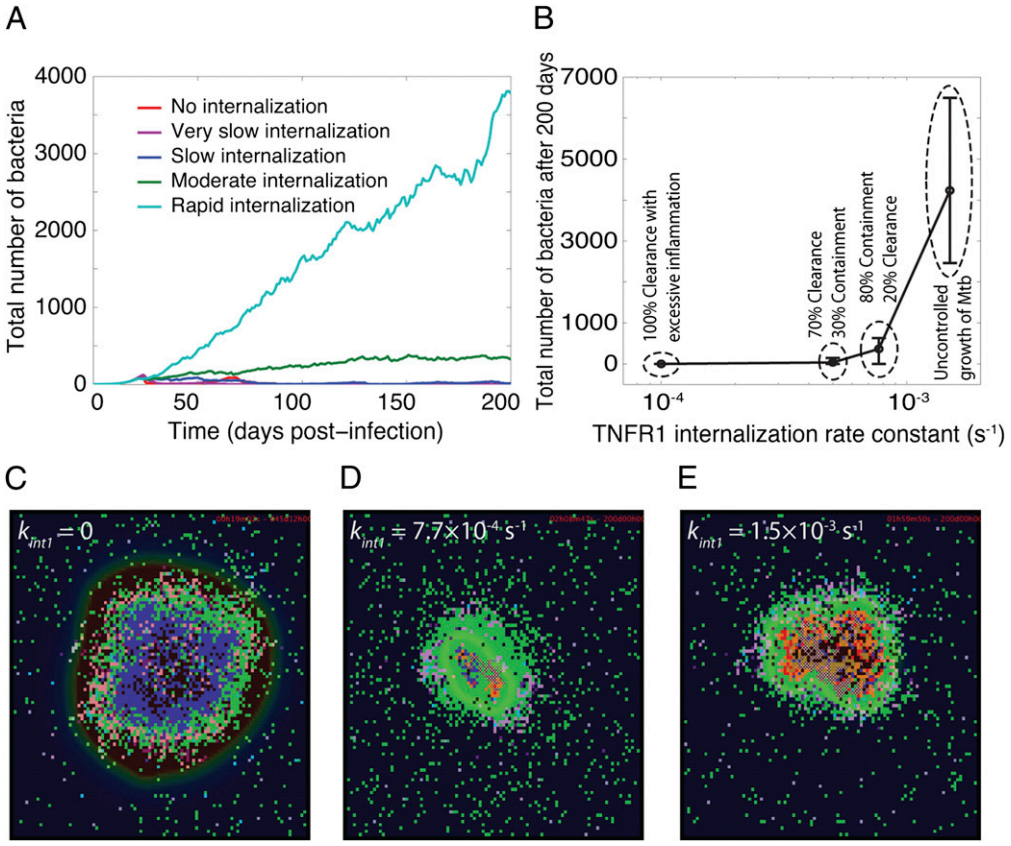

FIGURE 4. TNFR1 internalization dynamics control bacterial load during *M. tuberculosis* infection. Simulation results show (*A*) *M. tuberculosis* dynamics within a 200-d period after *M. tuberculosis* infection, (*B*) granuloma outcomes and bacterial load 200 d postinfection, (*C*) granuloma snapshot at the time of *M. tuberculosis* clearance (day 45) in the absence of TNFR1 internalization ($k_{int1} = 0$), (*D*, *E*) granuloma snapshots 200 d after *M. tuberculosis* infection for moderate ($k_{int1} = 7.7 \times 10^{-4}$ s^{-1}) and rapid ($k_{int1} = 1.5 \times 10^{-3}$ s^{-1}) rates of TNFR1 internalization. The colors representing cells of different type and status in granuloma snapshots are the same as those shown and defined in Fig. 2.

time of ~7.7 min, $k_{int1} = 1.5 \times 10^{-3}$ s^{-1}), infected macrophages become the main responders to TNF-α–induced activities ($R_{apoptosis}$ and $R_{NF\text{-}\kappa B} >> 1$). Fig. 6*C*–*F* displays how granulomas are affected by the rate at which sTNF–TNFR1 complexes become internalized; these snapshots are taken early after T cell recruitment to the site of infection. While a significant fraction of resting macrophages surrounding the infected core of granuloma become activated as a result of slow rates of TNFR1 internalization (i.e., there is a greater spatial range of TNF-α action, as seen in Fig. 6*C*), only a small number of infected macrophages in the core may become activated with a rapid rate of TNFR1 internalization (Fig. 6*F*). Thus, we suggest that the spatial range of TNF-α action within a granuloma is an important factor that controls the effect of TNFR1 internalization on the bacterial outcome of *M. tuberculosis* infection as well as the level of inflammation in the tissue.

A robust metric for assessing TNF-α impact on granuloma function

In the previous section, we demonstrated that the impact of the rate of TNFR1 internalization on bacterial levels in a granuloma is significantly correlated with infection status of macrophages that undergo TNF-α–mediated apoptosis or NF-κB activation ($R_{apoptosis}$ and $R_{NF\text{-}\kappa B}$). We explored the possibility that such a correlation between TNF-α activities and infection outcome also exists for other processes. We analyzed the effect of varying values of important TNF-α–associated molecular scale and linking parameters on $R_{apoptosis}$ and $R_{NF\text{-}\kappa B}$ during a 200-d period postinfection. A significant correlation was observed between bacterial levels and infected/resting cell ratios, $R_{apoptosis}$ and $R_{NF\text{-}\kappa B}$. As indicated in Fig. 7, an increase of one order of magnitude in cell surface sTNF–TNFR1 concentration threshold for NF-κB activation and TNF-α degradation rate constant or a decrease of one order of magnitude in NF-κB activation rate constant and the rate of mTNF synthesis by macrophages around baseline parameter values led to significant increases in both $R_{apoptosis}$ and $R_{NF\text{-}\kappa B}$ as well as bacterial levels. Outcomes of uncontrolled growth of *M. tuberculosis* generally occur at $R_{apoptosis}$ and $R_{NF\text{-}\kappa B}$ values of 1–10 or greater, and the chance of achieving clearance is greater for smaller values of these ratios. However, as indicated in Fig. 7*E*, when macrophage TNFR1 density is varied, the correlation between these ratios and bacterial levels (in clearance and containment cases in particular) does not appear very significant. This is probably because TNFR1 density has contradictory effects on TNF-α functions; although greater TNFR1 densities lead to more sensitive responses to smaller TNF-α concentrations, at the same time such larger densities enhance TNF-α uptake by macrophages limiting TNF-α availability in a granuloma. Overall, we suggest that infected/resting cell ratios we introduced in this study to compare TNF-α effects on infected versus resting macrophages, $R_{apoptosis}$ and $R_{NF\text{-}\kappa B}$, translate the effects of a variety of TNF-α–associated processes to granuloma outcomes.

Discussion

TNF-α was long suggested, based on experimental data from mice, to be essential for formation of granulomas in response to *M. tuberculosis* (17, 26, 70). However, recent TNFR1 knockout and TNF-α neutralization experiments in zebrafish and nonhuman primate models have shown that TNF-α, although not required for

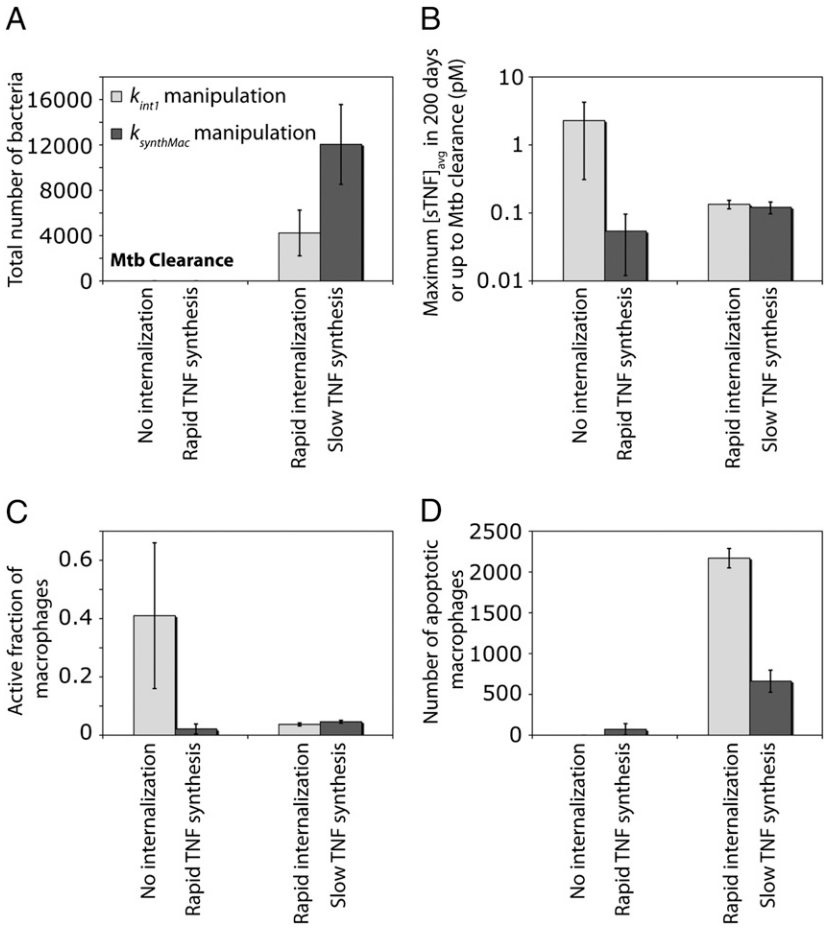

FIGURE 5. Manipulations in the rate constants for TNFR1 internalization (k_{int1}) and mTNF synthesis ($k_{synthMac}$) lead to different effects on model outputs. Simulation results show the effect of manipulations in k_{int1} and $k_{synthMac}$ on (*A*) bacterial levels 200 d after *M. tuberculosis* infection, (*B*) maximum sTNF concentration, (*C*) maximum fraction of macrophages that become activated after *M. tuberculosis* infection, and (*D*) TNF-α–induced macrophage apoptosis within a 200-d period after *M. tuberculosis* infection. No internalization, $k_{int1} = 0$; rapid TNF-α synthesis, $k_{synthMac} = 1$ #/cell-sec; rapid internalization, $k_{int1} = 1.5 \times 10^{-3}$ s^{-1}; slow TNF-α synthesis, $k_{synthMac} = 0.1$ #/cell-sec.

the formation of a granuloma, is important to restrict mycobacterial growth in a granuloma (27, 71). This suggests that TNF-α activities *within* a granuloma determine our ability to control *M. tuberculosis* infection. The important questions are, then, how TNF-α activities influence granuloma function, and what mechanisms control TNF-α activities in a granuloma during a long-term immune response to *M. tuberculosis*? To answer these questions, we need information about the spatial and temporal dynamics of TNF-α concentration during granuloma development in vivo. These experiments are not at present feasible, and thus these questions have remained unanswered. In this study, we use computational modeling/systems biology to address these questions. Our novel hypothesis is that events at different biological scales (molecular, cellular, and tissue scales) may influence TNF-

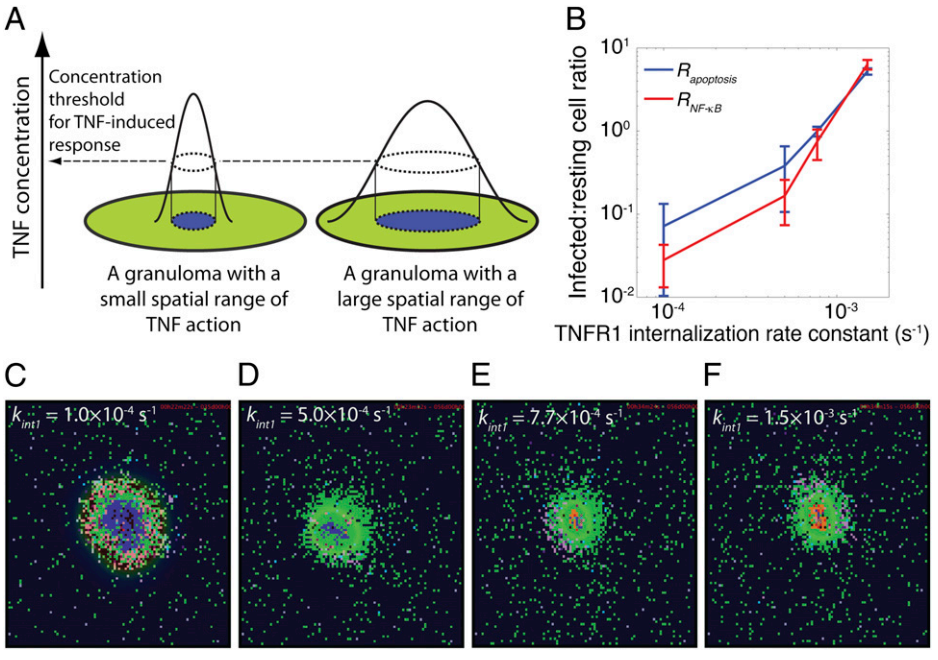

FIGURE 6. TNFR1 internalization dynamics control the spatial range of TNF-α action within a granuloma. *A*, Schematic definition of spatial range of TNF-α action in a granuloma. *B*, The effect of k_{int1} on $R_{apoptosis}$ and $R_{NF-κB}$, the ratios of total number of TNF-α–induced (apoptotic and NF-κB activated) infected macrophages to the number of TNF-α–induced resting macrophages within a 200-d period after *M. tuberculosis* infection. *C–F*, Granuloma snapshots early after recruitment of T cells for very slow, slow, medium, and rapid rates of sTNF-induced TNFR1 internalization. Simulated granuloma snapshots are shown at 5 wk after *M. tuberculosis* infection, right before clearance of bacteria in *C* and at 8 wk after *M. tuberculosis* infection in *D–F*. The colors representing cells of different type and status in granuloma snapshots are the same as those shown and defined in Fig. 2.

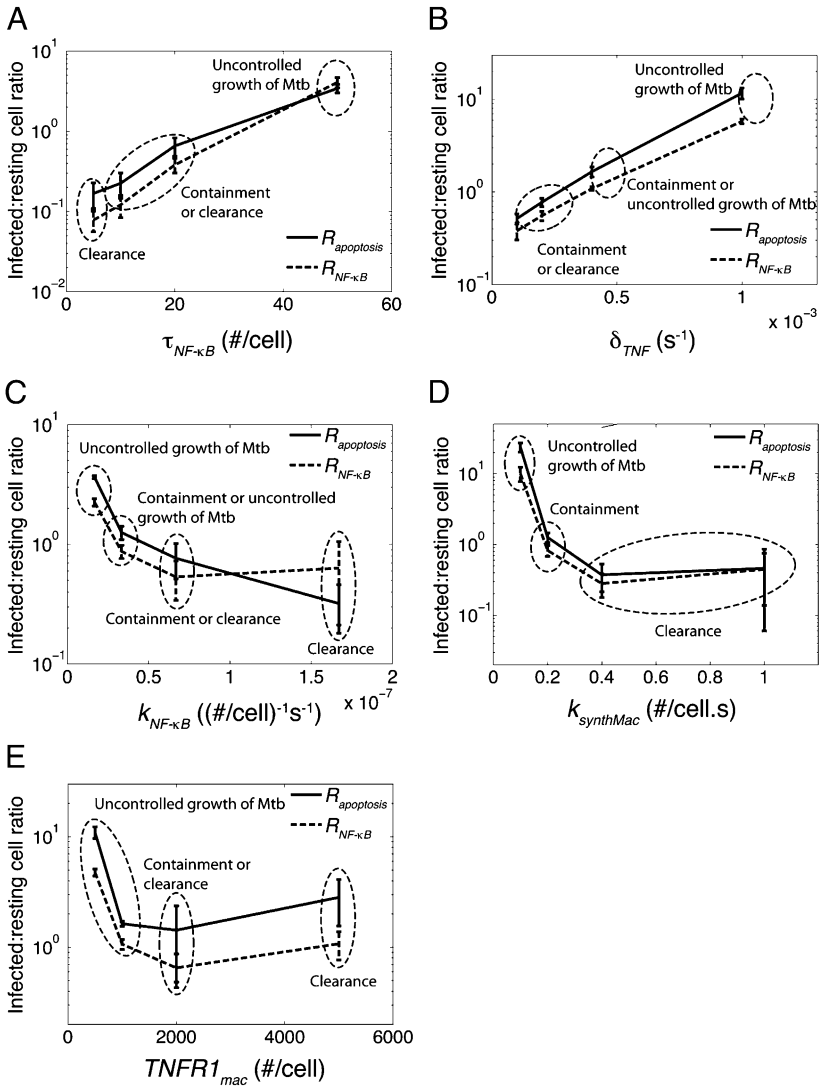

FIGURE 7. The impact of processes associated with TNF-α–TNFR on granuloma outcome is correlated with infection status of macrophages that undergo TNF-α–mediated apoptosis or NF-κB activation. Simulation results show the effect of (*A*) cell surface sTNF–TNFR1 concentration threshold for NF-κB activation ($\tau_{NF\text{-}\kappa B}$), (*B*) sTNF degradation rate constant (δ_{TNF}), (*C*) NF-κB activation rate constant ($k_{NF\text{-}\kappa B}$), (*D*) rate of mTNF synthesis by macrophages ($k_{synthMac}$), and (*E*) macrophage TNFR1 density ($TNFR1_{mac}$) on infected/resting cell ratios $R_{apoptosis}$ and $R_{NF\text{-}\kappa B}$ within a 200-d period after *M. tuberculosis* infection. Also indicated is granuloma outcome (clearance, containment, or uncontrolled growth of *M. tuberculosis*).

α activities in a granuloma, ultimately determining a granuloma's ability to control infection and inflammation. To address this hypothesis, our model was developed to link the dynamics of molecular scale TNF-α–TNFR interactions that occur on the second to minute timescales to cellular/tissue scale events that control the long-term immune response to *M. tuberculosis*. One of our interesting findings is that both TNF-α–independent cellular/tissue scale events (e.g., T cell recruitment or chemotactic movement of immune cells) and TNF-α–associated molecular scale processes (e.g., mTNF synthesis or TNFR1 internalization) influence TNF-α availability and activity in the granuloma, but in different ways. TNF-α–independent cellular scale processes influence bacterial numbers, and that controls TNF-α availability. However, TNF-α–associated molecular scale processes directly affect TNF-α availability and activities that control both the level of inflammation and bacterial numbers. Thus, there is an interplay between TNF-α availability and bacterial population at the site of infection that is controlled by the combined effects of molecular and cellular scale processes. An equilibrium state in this interplay leads to control of infection within a granuloma.

Our model reveals for the first time, to our knowledge, the importance of TNF-α–associated molecular processes (TNFR1 internalization in particular) in immunity to *M. tuberculosis*. We found that TNFR1 internalization regulates a balance between paracrine and autocrine TNF-α–induced responses, including NF-κB activation and apoptosis, in resting versus infected macrophages. Because resting macrophages do not express TNF, they become activated by TNF-α–producing cells only in a paracrine manner. However, infected macrophages express and release TNF-α to the extracellular space. Hence, they can become activated under the effect of TNF-α via both autocrine and paracrine pathways. Our results show that TNFR1 internalization favors activation of infected macrophages in an autocrine manner by restricting the diffusion of TNF-α from TNF-α–producing cells. TNF-α–induced activation of resting macrophages in addition to infected macrophages is necessary for controlling *M. tuberculosis* infection. Uncontrolled activation of resting macrophages, in contrast, may result in excessive inflammation. Thus, a balance between the autocrine and paracrine TNF-α–induced responses is required for an efficient granuloma response to *M. tuberculosis*, and an optimum rate of TNFR1 internalization can provide this balance. This finding can be considered in future studies examining approaches to control and therapy of TB or inhibition of TB reactivation, as several ways have already been proposed to influence the rate of TNFR1 internalization in vitro (42, 72, 73).

Another novel hypothesis from this study is that the efficacy of TNF-α in controlling *M. tuberculosis* infection is strongly affected by whether macrophages induced by TNF-α–mediated signaling pathways (NF-κB activation and apoptosis) are infected. Bacterial numbers are positively correlated with the ratio of infected

macrophages to (uninfected) resting macrophages that become activated by TNF-α. Thus, we suggest that this ratio is a critical factor that controls the outcome of *M. tuberculosis* infection at the granuloma level. This might be of particular interest in the case of TB reactivation as a result of using TNF-α–neutralizing drugs (e.g., for treatment of inflammatory diseases such as rheumatoid arthritis and Crohn's disease). As drug penetrates into a granuloma, resting macrophages, compared with infected macrophages in the granuloma core, are exposed to smaller concentrations of TNF-α and are affected by higher concentrations of the drug. This can potentially impair TNF-α function, leading to TB reactivation.

Finally, our findings may predict new therapies for control of TB as they suggest novel host targets (e.g., TNFR1 internalization and NF-κB activation) that play key roles in control of *M. tuberculosis* immune response. Further modeling studies including molecular detail of additional processes, such as those involving other cytokines (e.g., IL-10, IL-6, and IL-12) and chemokines, and using a similar approach to that identified in this study may also identify other important targets for therapy. Our multiscale computational model also provides a platform at the level of single granuloma to identify and compare therapeutic strategies as well as to investigate mechanisms by which TNF-α–neutralizing drugs (used to treat inflammatory diseases) or other drugs that diffuse in TB lesions may interfere with immune response to *M. tuberculosis* and reactivate TB.

Acknowledgments

We thank Joe Waliga for management of supporting materials at http://malthus.micro.med.umich.edu/lab/movies/Multiscale/GranSim/. We also thank JoAnne Flynn for helpful discussions.

Disclosures

The authors have no financial conflicts of interest.

References

1. Mortellaro, A., L. Robinson, and P. Ricciardi-Castagnoli. 2009. Spotlight on mycobacteria and dendritic cells: will novel targets to fight tuberculosis emerge? *EMBO Mol. Med.* 1: 19–29.
2. Russell, D. G., C. E. Barry, III, and J. L. Flynn. 2010. Tuberculosis: what we don't know can, and does, hurt us. *Science* 328: 852–856.
3. Lin, P. L., and J. L. Flynn. 2010. Understanding latent tuberculosis: a moving target. *J. Immunol.* 185: 15–22.
4. Algood, H. M., J. Chan, and J. L. Flynn. 2003. Chemokines and tuberculosis. *Cytokine Growth Factor Rev.* 14: 467–477.
5. Morel, P. A., S. Ta'asan, B. F. Morel, D. E. Kirschner, and J. L. Flynn. 2006. New insights into mathematical modeling of the immune system. *Immunol. Res.* 36: 157–165.
6. Davis, J. M., and L. Ramakrishnan. 2008. "The very pulse of the machine": the tuberculous granuloma in motion. *Immunity* 28: 146–148.
7. Tsai, M. C., S. Chakravarty, G. Zhu, J. Xu, K. Tanaka, C. Koch, J. Tufariello, J. Flynn, and J. Chan. 2006. Characterization of the tuberculous granuloma in murine and human lungs: cellular composition and relative tissue oxygen tension. *Cell. Microbiol.* 8: 218–232.
8. Ulrichs, T., G. A. Kosmiadi, V. Trusov, S. Jörg, L. Pradl, M. Titukhina, V. Mishenko, N. Gushina, and S. H. Kaufmann. 2004. Human tuberculous granulomas induce peripheral lymphoid follicle-like structures to orchestrate local host defence in the lung. *J. Pathol.* 204: 217–228.
9. Lin, P. L., S. Pawar, A. Myers, A. Pegu, C. Fuhrman, T. A. Reinhart, S. V. Capuano, E. Klein, and J. L. Flynn. 2006. Early events in *Mycobacterium tuberculosis* infection in cynomolgus macaques. *Infect. Immun.* 74: 3790–3803.
10. Turner, O. C., R. J. Basaraba, A. A. Frank, and I. M. Orme. 2003. Granuloma formation in mouse and guinea pig models of experimental tuberculosis. In *Granulomatous Infections and Inflammations: Cellular and Molecular Mechanisms*, 1st ed. . D. L. Boros, ed. ASM Press, Washington, DC, p. 65–84.
11. Barry, C. E., III, H. I. Boshoff, V. Dartois, T. Dick, S. Ehrt, J. Flynn, D. Schnappinger, R. J. Wilkinson, and D. Young. 2009. The spectrum of latent tuberculosis: rethinking the biology and intervention strategies. *Nat. Rev. Microbiol.* 7: 845–855.
12. Kirschner, D. E., D. Young, and J. L. Flynn. 2010. Tuberculosis: global approaches to a global disease. *Curr. Opin. Biotechnol.* 21: 524–531.
13. Flynn, J. L. 2004. Immunology of tuberculosis and implications in vaccine development. *Tuberculosis (Edinb.)* 84: 93–101.
14. Cooper, A. M. 2009. Cell-mediated immune responses in tuberculosis. *Annu. Rev. Immunol.* 27: 393–422.
15. Hanlon, A. M., S. Jang, and P. Salgame. 2002. Signaling from cytokine receptors that affect Th1 responses. *Front. Biosci.* 7: d1247–d1254.
16. Lauffenburger, D., and J. J. Linderman. 1993. *Receptors: Models for Binding, Trafficking, and Signaling.* Oxford University Press, New York.
17. Flynn, J. L., M. M. Goldstein, J. Chan, K. J. Triebold, K. Pfeffer, C. J. Lowenstein, R. Schreiber, T. W. Mak, and B. R. Bloom. 1995. Tumor necrosis factor-alpha is required in the protective immune response against *Mycobacterium tuberculosis* in mice. *Immunity* 2: 561–572.
18. Saunders, B. M., H. Briscoe, and W. J. Britton. 2004. T cell-derived tumour necrosis factor is essential, but not sufficient, for protection against *Mycobacterium tuberculosis* infection. *Clin. Exp. Immunol.* 137: 279–287.
19. Harris, J., J. C. Hope, and J. Keane. 2008. Tumor necrosis factor blockers influence macrophage responses to *Mycobacterium tuberculosis. J. Infect. Dis.* 198: 1842–1850.
20. Gutierrez, M. G., B. B. Mishra, L. Jordao, E. Elliott, E. Anes, and G. Griffiths. 2008. NF-kappa B activation controls phagolysosome fusion-mediated killing of mycobacteria by macrophages. *J. Immunol.* 181: 2651–2663.
21. Mosser, D. M., and J. P. Edwards. 2008. Exploring the full spectrum of macrophage activation. *Nat. Rev. Immunol.* 8: 958–969.
22. Zhou, Z., M. C. Connell, and D. J. MacEwan. 2007. TNFR1-induced NF-kappaB, but not ERK, p38MAPK or JNK activation, mediates TNF-induced ICAM-1 and VCAM-1 expression on endothelial cells. *Cell. Signal.* 19: 1238–1248.
23. Algood, H. M., P. L. Lin, D. Yankura, A. Jones, J. Chan, and J. L. Flynn. 2004. TNF influences chemokine expression of macrophages in vitro and that of CD11b+ cells in vivo during *Mycobacterium tuberculosis* infection. *J. Immunol.* 172: 6846–6857.
24. Keane, J., B. Shurtleff, and H. Kornfeld. 2002. TNF-dependent BALB/c murine macrophage apoptosis following *Mycobacterium tuberculosis* infection inhibits bacillary growth in an IFN-gamma independent manner. *Tuberculosis (Edinb.)* 82: 55–61.
25. Keane, J., M. K. Balcewicz-Sablinska, H. G. Remold, G. L. Chupp, B. B. Meek, M. J. Fenton, and H. Kornfeld. 1997. Infection by *Mycobacterium tuberculosis* promotes human alveolar macrophage apoptosis. *Infect. Immun.* 65: 298–304.
26. Chakravarty, S. D., G. Zhu, M. C. Tsai, V. P. Mohan, S. Marino, D. E. Kirschner, L. Huang, J. Flynn, and J. Chan. 2008. Tumor necrosis factor blockade in chronic murine tuberculosis enhances granulomatous inflammation and disorganizes granulomas in the lungs. *Infect. Immun.* 76: 916–926.
27. Lin, P. L., A. Myers, L. Smith, C. Bigbee, M. Bigbee, C. Fuhrman, H. Grieser, I. Chiosea, N. N. Voitenek, S. V. Capuano, et al. 2010. Tumor necrosis factor neutralization results in disseminated disease in acute and latent *Mycobacterium tuberculosis* infection with normal granuloma structure in a cynomolgus macaque model. *Arthritis Rheum.* 62: 340–350.
28. Roach, D. R., A. G. Bean, C. Demangel, M. P. France, H. Briscoe, and W. J. Britton. 2002. TNF regulates chemokine induction essential for cell recruitment, granuloma formation, and clearance of mycobacterial infection. *J. Immunol.* 168: 4620–4627.
29. Marino, S., D. Sud, H. Plessner, P. L. Lin, J. Chan, J. L. Flynn, and D. E. Kirschner. 2007. Differences in reactivation of tuberculosis induced from anti-TNF treatments are based on bioavailability in granulomatous tissue. *PLoS Comput. Biol.* 3: 1909–1924.
30. Ray, J. C., J. L. Flynn, and D. E. Kirschner. 2009. Synergy between individual TNF-dependent functions determines granuloma performance for controlling *Mycobacterium tuberculosis* infection. *J. Immunol.* 182: 3706–3717.
31. Fallahi-Sichani, M., M. A. Schaller, D. E. Kirschner, S. L. Kunkel, and J. J. Linderman. 2010. Identification of key processes that control tumor necrosis factor availability in a tuberculosis granuloma. *PLoS Comput. Biol.* 6: e1000778.
32. Warrender, C., S. Forrest, and F. Koster. 2006. Modeling intercellular interactions in early *Mycobacterium* infection. *Bull. Math. Biol.* 68: 2233–2261.
33. Pedrosa, J., B. M. Saunders, R. Appelberg, I. M. Orme, M. T. Silva, and A. M. Cooper. 2000. Neutrophils play a protective nonphagocytic role in systemic *Mycobacterium tuberculosis* infection of mice. *Infect. Immun.* 68: 577–583.
34. Seiler, P., P. Aichele, S. Bandermann, A. E. Hauser, B. Lu, N. P. Gerard, C. Gerard, S. Ehlers, H. J. Mollenkopf, and S. H. Kaufmann. 2003. Early granuloma formation after aerosol *Mycobacterium tuberculosis* infection is regulated by neutrophils via CXCR3-signaling chemokines. *Eur. J. Immunol.* 33: 2676–2686.
35. Zhang, X., L. Majlessi, E. Deriaud, C. Leclerc, and R. Lo-Man. 2009. Coactivation of Syk kinase and MyD88 adaptor protein pathways by bacteria promotes regulatory properties of neutrophils. *Immunity* 31: 761–771.
36. Zhu, X. W., and J. S. Friedland. 2006. Multinucleate giant cells and the control of chemokine secretion in response to *Mycobacterium tuberculosis. Clin. Immunol.* 120: 10–20.
37. Lay, G., Y. Poquet, P. Salek-Peyron, M. P. Puissegur, C. Botanch, H. Bon, F. Levillain, J. L. Duteyrat, J. F. Emile, and F. Altare. 2007. Langhans giant cells from *M. tuberculosis*-induced human granulomas cannot mediate mycobacterial uptake. *J. Pathol.* 211: 76–85.
38. Uehira, K., R. Amakawa, T. Ito, K. Tajima, S. Naitoh, Y. Ozaki, T. Shimizu, K. Yamaguchi, Y. Uemura, H. Kitajima, et al. 2002. Dendritic cells are decreased in blood and accumulated in granuloma in tuberculosis. *Clin. Immunol.* 105: 296–303.

39. Giri, P. K., and J. S. Schorey. 2008. Exosomes derived from M. Bovis BCG infected macrophages activate antigen-specific CD4+ and CD8+ T cells in vitro and in vivo. *PLoS ONE* 3: e2461.
40. Ordway, D., M. Henao-Tamayo, I. M. Orme, and M. Gonzalez-Juarrero. 2005. Foamy macrophages within lung granulomas of mice infected with *Mycobacterium tuberculosis* express molecules characteristic of dendritic cells and antiapoptotic markers of the TNF receptor-associated factor family. *J. Immunol.* 175: 3873–3881.
41. Peyron, P., J. Vaubourgeix, Y. Poquet, F. Levillain, C. Botanch, F. Bardou, M. Daffé, J. F. Emile, B. Marchou, P. J. Cardona, et al. 2008. Foamy macrophages from tuberculous patients' granulomas constitute a nutrient-rich reservoir for *M. tuberculosis* persistence. *PLoS Pathog.* 4: e1000204.
42. Schütze, S., T. Machleidt, D. Adam, R. Schwandner, K. Wiegmann, M. L. Kruse, M. Heinrich, M. Wickel, and M. Krönke. 1999. Inhibition of receptor internalization by monodansylcadaverine selectively blocks p55 tumor necrosis factor receptor death domain signaling. *J. Biol. Chem.* 274: 10203–10212.
43. Schneider-Brachert, W., V. Tchikov, J. Neumeyer, M. Jakob, S. Winoto-Morbach, J. Held-Feindt, M. Heinrich, O. Merkel, M. Ehrenschwender, D. Adam, et al. 2004. Compartmentalization of TNF receptor 1 signaling: internalized TNF receptosomes as death signaling vesicles. *Immunity* 21: 415–428.
44. Schütze, S., V. Tchikov, and W. Schneider-Brachert. 2008. Regulation of TNFR1 and CD95 signalling by receptor compartmentalization. *Nat. Rev. Mol. Cell Biol.* 9: 655–662.
45. Gupta, S. 2002. A decision between life and death during TNF-alpha-induced signaling. *J. Clin. Immunol.* 22: 185–194.
46. Saunders, B. M., S. Tran, S. Ruuls, J. D. Sedgwick, H. Briscoe, and W. J. Britton. 2005. Transmembrane TNF is sufficient to initiate cell migration and granuloma formation and provide acute, but not long-term, control of *Mycobacterium tuberculosis* infection. *J. Immunol.* 174: 4852–4859.
47. Fremond, C., N. Allie, I. Dambuza, S. I. Grivennikov, V. Yeremeev, V. F. Quesniaux, M. Jacobs, and B. Ryffel. 2005. Membrane TNF confers protection to acute mycobacterial infection. *Respir. Res.* 6: 136.
48. Olleros, M. L., R. Guler, D. Vesin, R. Parapanov, G. Marchal, E. Martinez-Soria, N. Corazza, J. C. Pache, C. Mueller, and I. Garcia. 2005. Contribution of transmembrane tumor necrosis factor to host defense against *Mycobacterium* bovis bacillus Calmette-Guerin and *Mycobacterium tuberculosis* infections. *Am. J. Pathol.* 166: 1109–1120.
49. Tay, S., J. J. Hughey, T. K. Lee, T. Lipniacki, S. R. Quake, and M. W. Covert. 2010. Single-cell NF-kappaB dynamics reveal digital activation and analogue information processing. *Nature* 466: 267–271.
50. Marino, S., I. B. Hogue, C. J. Ray, and D. E. Kirschner. 2008. A methodology for performing global uncertainty and sensitivity analysis in systems biology. *J. Theor. Biol.* 254: 178–196.
51. Fotin-Mleczek, M., F. Henkler, D. Samel, M. Reichwein, A. Hausser, I. Parmryd, P. Scheurich, J. A. Schmid, and H. Wajant. 2002. Apoptotic crosstalk of TNF receptors: TNF-R2-induces depletion of TRAF2 and IAP proteins and accelerates TNF-R1-dependent activation of caspase-8. *J. Cell Sci.* 115: 2757–2770.
52. Rangamani, P., and L. Sirovich. 2007. Survival and apoptotic pathways initiated by TNF-alpha: modeling and predictions. *Biotechnol. Bioeng.* 97: 1216–1229.
53. Blower, S. M., and H. Dowlatabadi. 1994. Sensitivity and uncertainty analysis of complex models of disease transmission: an HIV model, as an example. *Int. Stat. Rev.* 62: 229–243.
54. Bold, T. D., and J. D. Ernst. 2009. Who benefits from granulomas, mycobacteria or host? *Cell* 136: 17–19.
55. Lazarevic, V., D. Nolt, and J. L. Flynn. 2005. Long-term control of *Mycobacterium tuberculosis* infection is mediated by dynamic immune responses. *J. Immunol.* 175: 1107–1117.
56. Lin, P. L., M. Rodgers, L. Smith, M. Bigbee, A. Myers, C. Bigbee, I. Chiosea, S. V. Capuano, C. Fuhrman, E. Klein, and J. L. Flynn. 2009. Quantitative comparison of active and latent tuberculosis in the cynomolgus macaque model. *Infect. Immun.* 77: 4631–4642.
57. Flynn, J. L., and J. Chan. 2001. Immunology of tuberculosis. *Annu. Rev. Immunol.* 19: 93–129.
58. Sada-Ovalle, I., A. Chiba, A. Gonzales, M. B. Brenner, and S. M. Behar. 2008. Innate invariant NKT cells recognize *Mycobacterium tuberculosis*-infected macrophages, produce interferon-gamma, and kill intracellular bacteria. *PLoS Pathog.* 4: e1000239.
59. Segovia-Juarez, J. L., S. Ganguli, and D. Kirschner. 2004. Identifying control mechanisms of granuloma formation during *M. tuberculosis* infection using an agent-based model. *J. Theor. Biol.* 231: 357–376.
60. Theus, S., K. Eisenach, N. Fomukong, R. F. Silver, and M. D. Cave. 2007. Beijing family *Mycobacterium tuberculosis* strains differ in their intracellular growth in THP-1 macrophages. *Int. J. Tuberc. Lung Dis.* 11: 1087–1093.
61. Lin, P. L., H. L. Plessner, N. N. Voitenok, and J. L. Flynn. 2007. Tumor necrosis factor and tuberculosis. *J. Investig. Dermatol. Symp. Proc.* 12: 22–25.
62. Keane, J., S. Gershon, R. P. Wise, E. Mirabile-Levens, J. Kasznica, W. D. Schwieterman, J. N. Siegel, and M. M. Braun. 2001. Tuberculosis associated with infliximab, a tumor necrosis factor alpha-neutralizing agent. *N. Engl. J. Med.* 345: 1098–1104.
63. Winthrop, K. L. 2006. Risk and prevention of tuberculosis and other serious opportunistic infections associated with the inhibition of tumor necrosis factor. *Nat. Clin. Pract. Rheumatol.* 2: 602–610.
64. Flynn, J. L. 2006. Lessons from experimental *Mycobacterium tuberculosis* infections. *Microbes Infect.* 8: 1179–1188.
65. Bean, A. G., D. R. Roach, H. Briscoe, M. P. France, H. Korner, J. D. Sedgwick, and W. J. Britton. 1999. Structural deficiencies in granuloma formation in TNF gene-targeted mice underlie the heightened susceptibility to aerosol *Mycobacterium tuberculosis* infection, which is not compensated for by lymphotoxin. *J. Immunol.* 162: 3504–3511.
66. Grell, M., H. Wajant, G. Zimmermann, and P. Scheurich. 1998. The type 1 receptor (CD120a) is the high-affinity receptor for soluble tumor necrosis factor. *Proc. Natl. Acad. Sci. USA* 95: 570–575.
67. Higuchi, M., and B. B. Aggarwal. 1994. TNF induces internalization of the p60 receptor and shedding of the p80 receptor. *J. Immunol.* 152: 3550–3558.
68. Bekker, L. G., A. L. Moreira, A. Bergtold, S. Freeman, B. Ryffel, and G. Kaplan. 2000. Immunopathologic effects of tumor necrosis factor alpha in murine mycobacterial infection are dose dependent. *Infect. Immun.* 68: 6954–6961.
69. Engele, M., E. Stössel, K. Castiglione, N. Schwerdtner, M. Wagner, P. Bölcskei, M. Röllinghoff, and S. Stenger. 2002. Induction of TNF in human alveolar macrophages as a potential evasion mechanism of virulent *Mycobacterium tuberculosis. J. Immunol.* 168: 1328–1337.
70. Algood, H. M., P. L. Lin, and J. L. Flynn. 2005. Tumor necrosis factor and chemokine interactions in the formation and maintenance of granulomas in tuberculosis. *Clin. Infect. Dis.* 41(Suppl 3): S189–S193.
71. Clay, H., H. E. Volkman, and L. Ramakrishnan. 2008. Tumor necrosis factor signaling mediates resistance to mycobacteria by inhibiting bacterial growth and macrophage death. *Immunity* 29: 283–294.
72. Schneider-Brachert, W., V. Tchikov, O. Merkel, M. Jakob, C. Hallas, M. L. Kruse, P. Groitl, A. Lehn, E. Hildt, J. Held-Feindt, et al. 2006. Inhibition of TNF receptor 1 internalization by adenovirus 14.7K as a novel immune escape mechanism. *J. Clin. Invest.* 116: 2901–2913.
73. Neumeyer, J., C. Hallas, O. Merkel, S. Winoto-Morbach, M. Jakob, L. Thon, D. Adam, W. Schneider-Brachert, and S. Schütze. 2006. TNF-receptor I defective in internalization allows for cell death through activation of neutral sphingomyelinase. *Exp. Cell Res.* 312: 2142–2153.